2021 American Control Conference (ACC)
New Orleans, USA, May 25-28, 2021

Saving Energy with Delayed Information in Connected Vehicle Systems

Minghao Shen[1], Tamás G. Molnár[1,2], Chaozhe R. He[1,3], A. Harvey Bell[1],
Matthew Hunkler[3], Dean Oppermann[3], Russell Zukouski[3], Jim Yan[3], and Gábor Orosz[1,4]

***Abstract*— In this paper, we design an energy-optimal longitudinal controller for connected automated trucks driving in mixed traffic with lean penetration of connected vehicles. The controller utilizes information received via vehicle-to-vehicle connectivity from vehicles traveling ahead of the truck, and additional delays are introduced into the control law to improve energy efficiency. We evaluate the robustness of the energy-optimal control parameters and calculate the amount of energy benefits. Simulation results show 18% improvement of energy efficiency compared to a non-connected design, and 3% improvement compared to the connected design without additional delay.**

I. Introduction

Heavy-duty vehicles take up a large proportion of today's freight transportation [1]. Improving fuel economy is therefore an important concern for these vehicles, as it brings significant financial [2] and environmental [3] benefits. A potential way to reduce fuel consumption is optimizing the longitudinal control of these vehicles. It has been shown that following an optimal velocity profile that is computed based on geographical information (such as elevation) can lead to significant fuel economy improvement in traffic-free environments [4], [5], while one may also obtain improvements in traffic with a careful control design [6].

The development of wireless vehicle-to-vehicle (V2V) communication technologies provides additional opportunities for improving fuel economy. Connectivity allows vehicles to obtain information from beyond line of sight [7], that has shown great potential for energy efficiency when utilized by connected automated vehicles [8], [9], [10]. Researchers therefore are actively investigating different solutions for exploiting connectivity and automation, such as centralized coordination [11] or cooperative adaptive cruise control [12]. Although some of these methods require large penetration of connectivity, which may be hard to achieve in practice, a small amount of connected vehicles on the road can already lead to benefits in safety and control performance [13], [14].

In this paper, we design longitudinal controller for connected automated trucks (CATs) by assuming lean penetration of connectivity. We show that CATs can save significant energy by responding to the motion of not only the immediate preceding vehicle, but also connected vehicles farther ahead. Moreover, we demonstrate that an immediate response to distant connected vehicles may not be the optimal strategy, but the CAT shall delay its response to achieve lower energy consumption. Thus, we introduce additional delay in the control law and, with some care, we use the delay as design parameter to improve energy efficiency while maintaining stability.

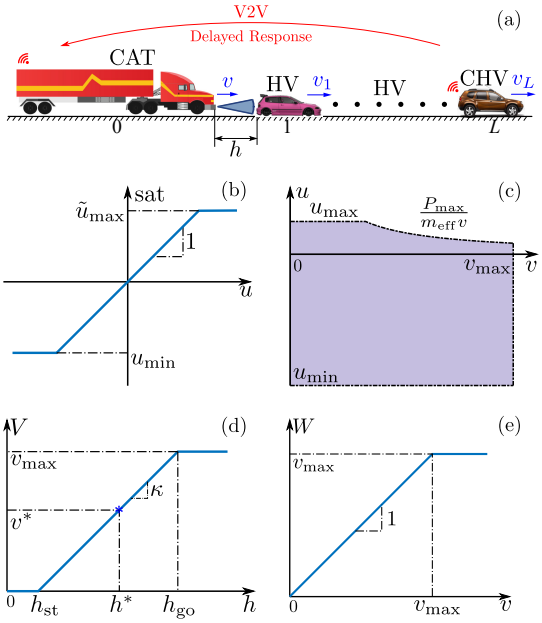

Fig. 1. (a) A connected automated truck in mixed traffic consisting of connected and non-connected human driven vehicles on a single lane road. (b,c) Saturation function in (3) with the limits given by (4). (d) Range policy in (7). (e) Saturation function in (8).

The paper is organized as follows. Section II proposes the longitudinal control design for CATs that utilizes delayed information from V2V communication while assuming lean penetration of connectivity. Section III describes a design paradigm to ensure the energy efficiency of this controller when responding to preceding traffic. To this end, an experimental dataset collected from human driven vehicles is used. Section IV evaluates the energy efficiency of the proposed controller and studies the robustness of the control design against using data from different leading vehicles. Section V summarizes the main conclusions.

II. Control Design

In this section, we design longitudinal controller for connected automated trucks (CATs) utilizing V2V communi-

This work was supported by Navistar, Inc.

[1]M. Shen, T. G. Molnár, A. H. Bell, C. R. He and G. Orosz are with the Department of Mechanical Engineering, University of Michigan, Ann Arbor, MI 48105, USA {mhshen, molnart, ahbelliv, orosz}@umich.edu

[2]C. R. He, M. Hunkler, D. Oppermann, R. Zukouski, and J. Yan are with Navistar, Inc. Lisle, IL 60532, USA {Chaozhe.He, Matthew.Hunkler, Dean.Oppermann, Russ.Zukouski, Jim.Yan} @navistar.com

[3]T. G. Molnár is also with the Department of Mechanical and Civil Engineering, California Institute of Technology, Pasadena, CA 91125, USA

[4]G. Orosz is also with the Department of Civil and Environmental Engineering, University of Michigan, Ann Arbor, MI 48109, USA

cation in mixed traffic with lean penetration of connected vehicles. Consider the car-following scenario in Fig. 1(a) where a CAT is driving in mixed traffic consisting of human-driven vehicles (HVs) and connected human-driven vehicles (CHVs). While the CAT may not be connected with all vehicles in traffic, we assume that the position and velocity of the vehicle immediately ahead (vehicle 1) is always available via on-board sensors (e.g., radar or LiDAR). Furthermore, we assume that the CAT receives information from at least one connected vehicle farther ahead (vehicle L, $L \geq 2$). We design a longitudinal controller utilizing the information about vehicle 1 and vehicle L.

A. Longitudinal dynamics

We model the longitudinal motion by

$$\begin{aligned} \dot{h}(t) &= v_1(t) - v(t), \\ \dot{v}(t) &= -f(v(t)) + \ \mathrm{sat}\big(u(t-\sigma)\big), \\ u(t) &= \tilde{f}(t) + a_{\mathrm{d}}(t) \end{aligned} \tag{1}$$

where v and v_1 are the speeds of the truck and the preceding vehicle and h is the distance headway between them. Here a_{d} denotes the desired acceleration of the truck calculated from higher level control command. The term

$$f(v) = \frac{1}{m_{\mathrm{eff}}}(\gamma m \mathrm{g} + k_0 v^2), \tag{2}$$

captures nonlinear physical effects of the air drag and rolling resistance [8]. Here m_{eff} is the effective mass given by $m_{\mathrm{eff}} = m + I/R^2$ containing the mass m of the truck, the inertia I of the wheels, and the tire radius R, while γ is the rolling resistance coefficient, g is the gravitational acceleration, and k_0 is the air drag coefficient. In order to cancel the resistance term $f(v)$, a compensation term $\tilde{f}(v)$ is often implemented by a lower level controller. For simplicity we assume the vehicles are traveling on flat road.

The overall control input $u(t)$ of the truck is subject to a time delay σ that models the delay in the powertrain system. The control input is limited by the braking torque (with corresponding limit $u_{\min}$), engine torque (associated with $u_{\max}$) and engine power $P_{\max}$ given by

$$\mathrm{sat}(u) = \begin{cases} u_{\min}, & \text{if } u \leq u_{\min} \\ u, & \text{if } u_{\min} < u < \tilde{u}_{\max} \\ \tilde{u}_{\max}, & \text{if } u \geq \tilde{u}_{\max} \end{cases}, \tag{3}$$

cf. Fig 1(b), where

$$\tilde{u}_{\max} = \min\left\{u_{\max}, \ \frac{P_{\max}}{m_{\mathrm{eff}} v}\right\}, \tag{4}$$

cf. Fig. 1(c).

To measure the energy consumption of the CAT, we define the overall energy consumption per unit mass over the time interval $t \in [t_0, t_{\mathrm{f}}]$:

$$w = \int_{t_0}^{t_{\mathrm{f}}} v(t)\, g\left(\dot{v}(t) + f(v(t))\right) \mathrm{d}t, \tag{5}$$

where $g(x) = \max\{x, 0\}$. Since w involves kinematic quantities only, it can be applied to both vehicles with internal combustion engine, electric vehicles or hybrid vehicles, with the appropriate choice of function g [10].

B. Connected cruise control with delayed information

The proposed longitudinal controller requests for a desired acceleration a_{d} in (1) as follows:

$$\begin{aligned} a_{\mathrm{d}}(t) = &\alpha\left(V(h(t)) - v(t)\right) \\ &+ \beta\left(W(v_1(t)) - v(t)\right) \\ &+ \hat{\beta}\left(W(v_L(t-\hat{\sigma})) - v(t)\right), \end{aligned} \tag{6}$$

where the first term keeps a desired headway of the CAT, the second term controls the CAT to match its speed with the speed of vehicle 1, while the third term responds to the speed v_L of vehicle L, with control gains α, β and $\hat{\beta}$, respectively. The range policy $V(\cdot)$ describes the desired velocity of the truck as a function of the headway in the form

$$V(h) = \begin{cases} 0, & \text{if } h \leq h_{\mathrm{st}}, \\ \kappa(h - h_{\mathrm{st}}), & \text{if } h_{\mathrm{st}} < h < h_{\mathrm{go}}, \\ v_{\max}, & \text{if } h \geq h_{\mathrm{go}}, \end{cases} \tag{7}$$

as shown in Fig. 1(d). For small headway $h \leq h_{\mathrm{st}}$, the truck tends to stop while for large headway $h \geq h_{\mathrm{go}}$, the truck tends to travel with maximum speed $v_{\max}$. For medium headway $h_{\mathrm{st}} < h < h_{\mathrm{go}}$, the desired velocity increases linearly (with gradient κ) as a function of the headway. Finally, the saturation function

$$W(v) = \begin{cases} v, & \text{if } v < v_{\max}, \\ v_{\max}, & \text{if } v \geq v_{\max}, \end{cases} \tag{8}$$

shown in Fig. 1(e) keeps the truck under the speed limit when following a speeding vehicle.

Note that an additional delay $\hat{\sigma} \geq 0$ is introduced in the response to the data v_L obtained from vehicle L via V2V connectivity. The intuition behind this is if vehicle L is far ahead (i.e., L is large), it may be beneficial to wait until the effect of its motion propagates through the subsequent vehicles closer to the CAT, rather than respond to its motion immediately. While delays are often undesired as they may lead to instability [15] and further safety hazard, they can also improve the stability margin under some circumstances [16]. Here we introduce additional delay in the feedback term of v_L only, and we will show that it improves energy efficiency while the stability of the closed-loop system can still be guaranteed.

C. Stability conditions for maintaining constant velocity

To study the stability of the closed-loop system with the proposed controller, we linearize system (1) with (6) around the uniform flow equilibrium given by

$$v(t) \equiv v_1(t) \equiv v_L(t) \equiv v^*, \quad h(t) \equiv h^*, \quad v^* = V(h^*). \tag{9}$$

Let us define the state perturbations $\tilde{h} = h - h^*$, $\tilde{v} = v - v^*$, $\tilde{v}_1 = v_1 - v^*$ and $\tilde{v}_L = v_L - v^*$, by which the linearized dynamics are expressed as

$$\begin{aligned} \dot{\tilde{h}}(t) =& \tilde{v}_1(t) - \tilde{v}(t), \\ \dot{\tilde{v}}(t) =& \alpha\left(\kappa\tilde{h}(t-\sigma) - \tilde{v}(t-\sigma)\right) \\ &+ \beta(\tilde{v}_1(t-\sigma) - \tilde{v}(t-\sigma)) \\ &+ \hat{\beta}\left(\tilde{v}_L(t-(\sigma+\hat{\sigma})) - \tilde{v}(t-\sigma)\right). \end{aligned} \tag{10}$$

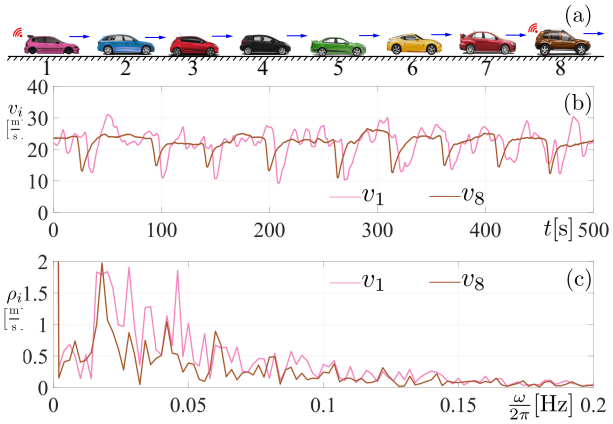

Fig. 2. (a) Eight connected human driven vehicles traveling on a single-lane road. (b) The velocity profile of leading vehicle 8 and tail vehicle 1. (c) The amplitude spectra of the velocity profiles of vehicle 8 and vehicle 1.

In order for the truck to be able to maintain constant speed around equilibrium (9), we require the linearized system (10) to be plant stable [17]. Plant stability can be analyzed by transforming (10) into Laplace domain

$$V(s) = T_{01}(s)V_1(s) + T_{0L}(s)V_L(s), \tag{11}$$

with transfer functions

$$\begin{aligned} T_{01}(s) &= \frac{\alpha\kappa + \beta s}{s^2 e^{s\sigma} + (\alpha+\beta+\hat{\beta})s + \alpha\kappa}, \\ T_{0L}(s) &= \frac{\hat{\beta} s e^{-s\hat{\sigma}}}{s^2 e^{s\sigma} + (\alpha+\beta+\hat{\beta})s + \alpha\kappa}. \end{aligned} \tag{12}$$

Plant stability is achieved when all roots of the characteristic equation

$$s^2 e^{s\sigma} + (\alpha+\beta+\hat{\beta})s + \alpha\kappa = 0 \tag{13}$$

have negative real parts. According to [17], the parameters $(\alpha, \beta, \hat{\beta})$ need to be selected from the region given by

$$\alpha > 0, \tag{14}$$

$$\underline{\omega}\sin(\underline{\omega}\sigma) - \alpha < \beta + \hat{\beta} < \overline{\omega}\sin(\overline{\omega}\sigma) - \alpha, \tag{15}$$

where $\underline{\omega}$ and $\overline{\omega}$ are the solutions of transcendental equation $\alpha\kappa = \omega^2\cos(\omega\sigma)$ such that $0 < \underline{\omega} < \overline{\omega} < \frac{\pi}{2}$. Notice that the introduction of the additional delay $\hat{\sigma}$ has no influence on plant stability.

III. Optimal Control Parameters Based on Data

In this section, we propose a method to determine the energy-optimal parameters of the proposed controller based on the data of the preceding vehicles using the frequency domain approach introduced in [10]. To motivate the design method, we use trajectory data recorded on human driven vehicles by the experiments described in [14]. During these experiments, eight connected human driven vehicles performed car-following in a single lane along a flat road; see Fig. 2(a). Each vehicle was equipped with V2V devices, and their position and speed were recorded via GPS. Our goal is to select the parameters of controller (6) so that a CAT can follow these eight vehicles in an energy efficient manner while it uses data only from vehicles 1 and L, $2 \le L \le 8$.

The experimental velocity data of vehicle 1 and vehicle 8 are plotted in Fig. 2(b). Vehicle 8 made a sequence of mild brakes while maintaining its average velocity around 20 [m/s]. Such mild brake actions led to more severe brake actions later by vehicle 1. This behavior, which is an example of string instability typically seen in human-driven vehicle chains, makes vehicle 1 waste energy by the excessive usage of braking. Notice that the braking actions of vehicle 1 and vehicle 8 usually have long time gaps between them, varying from 6 seconds to 10 seconds. This observation inspires the controller design for the CAT to delay its response to vehicle L if it is far ahead (i.e., if L is large, such as $L = 8$).

To confirm the correlation between vehicle 1 and the distant vehicle L, we write the velocity perturbations of vehicles 1 and L as Fourier series with M frequency components

$$\begin{aligned} \tilde{v}_1(t) &= \sum_{i=1}^{M} \rho_{1,i}\sin(\omega_i t + \varphi_{1,i}), \\ \tilde{v}_L(t) &= \sum_{i=1}^{M} \rho_{L,i}\sin(\omega_i t + \varphi_{L,i}). \end{aligned} \tag{16}$$

Here the frequencies are given as $\omega_i = i\Delta\omega$ where $\Delta\omega = \frac{2\pi}{t_f - t_0}$, while $\rho_{1,i}$, $\rho_{L,i}$ denote the corresponding amplitudes and $\varphi_{1,i}$, $\varphi_{L,i}$ indicate the phase angles. The Fourier spectra are illustrated for the data of vehicles 1 and 8 in Fig. 2(c). Indeed, both spectra contain major components in low frequency domain, they correlate well, and the signal of vehicle 1 contains larger values for most frequency components than that of vehicle 8.

Using the transfer functions (12) at $s = \mathrm{j}\omega_i$ ($\mathrm{j}^2 = -1$) and the spectra of v_1 and v_L, we acquire the steady state velocity response $\tilde{v}$ of the truck as :

$$\tilde{v}(t) = \sum_{i=1}^{M}\big(D_{1,i}\sin(\omega_i t + \theta_{1,i}) + D_{L,i}\sin(\omega_i t + \theta_{L,i})\big), \tag{17}$$

where

$$\begin{aligned} D_{1,i} &= \rho_{1,i}|T_{01}(\mathrm{j}\omega_i)|, \qquad \theta_{1,i} = \varphi_{1,i} + \angle T_{01}(\mathrm{j}\omega_i), \\ D_{L,i} &= \rho_{L,i}|T_{0L}(\mathrm{j}\omega_i)|, \qquad \theta_{L,j} = \varphi_{L,i} + \angle T_{0L}(\mathrm{j}\omega_i). \end{aligned} \tag{18}$$

By combining the trigonometric terms, we rewrite (17) as

$$\tilde{v}(t) = \sum_{i=1}^{M} D_i\sin(\omega_i t + \theta_i), \tag{19}$$

where

$$\begin{aligned} D_i &= \sqrt{C^2 + S^2}, \quad \tan\theta_i = S/C, \\ C &= D_{1,i}\cos\theta_{1,i} + D_{L,i}\cos\theta_{L,i}, \\ S &= D_{1,i}\sin\theta_{1,i} + D_{L,i}\sin\theta_{L,i}. \end{aligned} \tag{20}$$

Given a certain set of control parameters $(\alpha, \beta, \hat{\beta}, \hat{\sigma})$, one can calculate $\tilde{v}$, and then obtain the energy consumption w by (5), both as a function of the control parameters. The optimal design parameters are the ones that the give least energy consumption w. According to [10], the energy consumption

w can be upper and lower bounded by a class-$\mathcal{K}$ function of the cost function

$$J = \sum_{i=1}^{M} \omega_i^2 D_i^2. \tag{21}$$

Thus, minimizing J can give sub-optimal control parameters close to the ones that minimize w. We remark that the computation of J can be performed efficiently based on data and allows updating control parameters online. By contrast, getting w in (5) using actual response of the original nonlinear system (1,6) requires extensive numerical simulations over a large number of control parameter combinations, and thus, may only be acquired offline.

IV. Design Results

In this section we apply the design method proposed in the previous section and evaluate the control performance. Specifically, we simulate the scenario shown in Fig. 1 with the speed profiles of vehicles 1 and L taken from data (e.g., those of vehicle 1 and 8 shown in Fig. 2(b)). It is assumed that one of the seven vehicles ahead of vehicle 1 is connected to the truck via V2V communication, that is, $2 \leq L \leq 8$. We consider a fully-loaded heavy duty truck with parameters given by Table I according to [5] and we design the remaining control parameters $(\beta, \hat{\beta}, \hat{\sigma})$ such that the energy consumption is minimized.

TABLE I
Dynamical and control parameters of the CAT.

Parameter	Value	Parameter	Value
m	29484 [kg]	$v_{\max}$	30 [m/s]
m_{eff}	29641 [kg]	h_{st}	5 [m]
γ	0.006	h_{go}	55 [m]
k_0	3.84 [kg/m]	κ	0.6 [1/s]
$u_{\min}$	-4 [m/s^2]	α	0.4 [1/s]
$u_{\max}$	1 [m/s^2]	σ	0.6 [s]
$P_{\max}$	300.65 [kW]		

A. Benchmark: controllers with non-delayed information

To establish a benchmark for the proposed connected cruise controller, we consider two baseline controllers: adaptive cruise controller (ACC) and connected cruise controller (CCC) with non-delayed information.

Without V2V information, the truck responds to vehicle 1 only, which is referred as ACC. We consider the ACC control law as a special case of (6) with $\hat{\beta} = 0$, thus β is the only design parameter for ACC. To calculate the energy consumption per unit mass w for ACC, we vary β from 0 to 1 [1/s] with step size 0.05 [1/s], and we perform simulation of (1,6) for each β value. The resulting energy consumption is shown as a function of β in Fig. 3(a), where the minimum value of w is 3.73 [kJ/kg] is achieved for $\beta = 0.65$ [1/s].

With V2V connectivity, the truck can receive information from a distant vehicle and respond to both vehicle 1 and vehicle L, which is referred to as CCC. The control law for CCC with non-delayed information is (6) with $\hat{\sigma} = 0$, i.e., CCC has two design parameters: β and $\hat{\beta}$. Figure 3(b) shows the energy consumption w of CCC as a function of $\hat{\beta}$ for $L = 8$ with β being fixed to the optimal parameter value

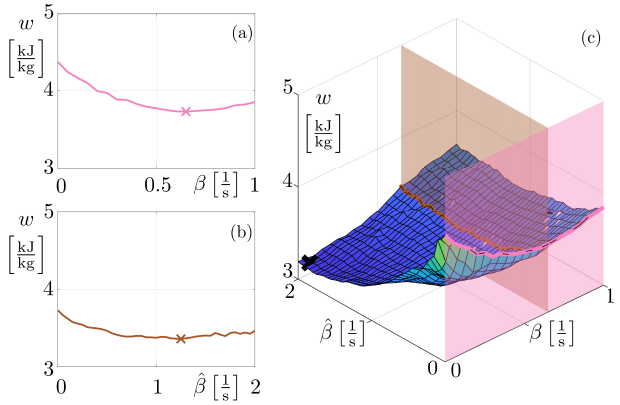

Fig. 3. Energy consumption of benchmark controllers using non-delayed information, i.e., (6) with $\hat{\sigma} = 0$. (a) Energy consumption of ACC as a function of β for $\hat{\beta} = 0$. (b) Energy consumption of CCC with non-delayed information as a function of $\hat{\beta}$ for $\beta = 0.65$ [1/s]. (c) Energy consumption of CCC with non-delayed information as a function of $(\beta, \hat{\beta})$. The optimal point is at the black dot with $(\beta, \hat{\beta}) = (0.05,\ 1.95)$ [1/s]. Pink and brown planes correspond to the sections in panels (a) and (b), respectively.

obtained for ACC, $\beta = 0.65$ [1/s]. The lowest w value is 3.36 [kJ/kg] at $\hat{\beta} = 1.25$ [1/s], which is 9.4% lower than that of ACC.

To explore the full performance spectrum of CCC, one can vary $(\beta, \hat{\beta})$ together. The surface depicted in Fig. 3(c) shows w as a function of $(\beta, \hat{\beta})$. We remark that the curves in Fig. 3(a) and Fig. 3(b) are the intersections of this surface with the pink plane $\hat{\beta} = 0$ and the brown plane $\beta = 0.65$ [1/s]. CCC is able to achieve a minimum w value of 3.16 [kJ/kg] at $(\beta, \hat{\beta}) = (0.05, 1.95)$ [1/s], which is 15.4% more efficient than ACC. This shows that energy efficiency can be improved significantly using extra information from V2V connectivity with just one vehicle farther ahead.

B. Benefits from delayed information

In this part we investigate the energy benefit brought by delaying the use of information from vehicles farther ahead. We vary three control parameters, β, $\hat{\beta}$ and $\hat{\sigma}$, to acquire the optimal energy consumption w. In particular, we fix $L = 8$ and we vary $(\beta, \hat{\beta})$ within the domain $[0, 1] \times [0, 2]$ with step size 0.05 [1/s] and $\hat{\sigma}$ within $[0, 5.5]$ with step size 0.1 [s].

Figure 4 plots the contours of w in the $(\beta, \hat{\beta})$ plane for various values of $\hat{\sigma}$. The energy contours are shown within the plant stable domain only, whose boundary (15) is indicated by red dashed line. Panel (a) shows the case without additional delay, $\hat{\sigma} = 0$, that corresponds to Fig. 3(c). Panels (b), (c) and (d) are associated with $\hat{\sigma} = 1.5$ [s], $\hat{\sigma} = 1.6$ [s] and $\hat{\sigma} = 3.7$ [s], respectively. The figure highlights that it is possible to reach lower energy levels by adding the delay $\hat{\sigma}$.

The energy-optimal control parameter for each $\hat{\sigma}$ is marked as black dots in Fig. 4. To illustrate the optimal parameters $(\beta^*, \hat{\beta}^*, \hat{\sigma}^*)$, we plot β^* and $\hat{\beta}^*$as a function of $\hat{\sigma}$ as depicted by the solid curves in Fig. 5(a). As $\hat{\sigma}$ is increased, there is a sudden change in the optimal control gains at a certain delay $\hat{\sigma}_{\text{cr}}$. This can be explained by the contour plots in Fig. 4. Around a critical value $\hat{\sigma} = \hat{\sigma}_{\text{cr}}$, highlighted by Fig. 4(b,c), there are two local minima in the contour plots:

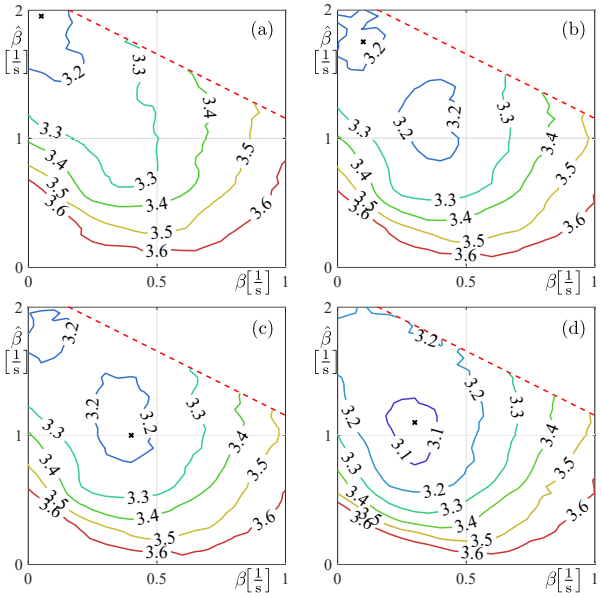

Fig. 4. Level sets of energy consumption per unit mass w in the $(\beta, \hat{\beta})$ plane with different $\hat{\sigma}$. Red dashed line corresponds to the plant stability boundary (15). (a) $\hat{\sigma} = 0$. (b) $\hat{\sigma} = 1.5$ [s]. (c) $\hat{\sigma} = 1.6$ [s]. (d) $\hat{\sigma} = 3.7$ [s].

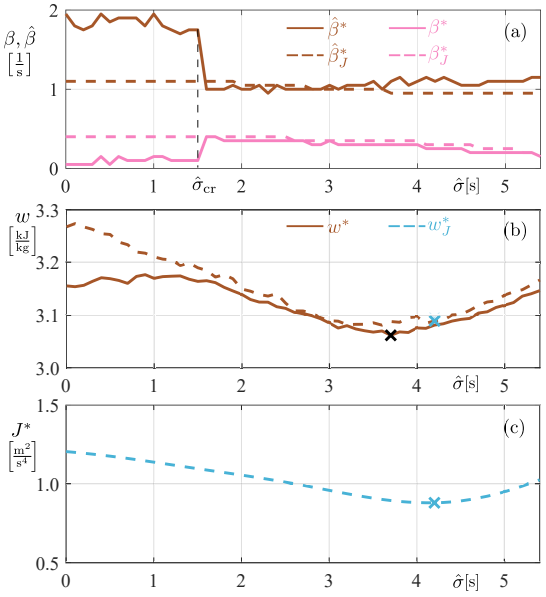

Fig. 5. Comparison between cost function-based design and optimal parameter choice. (a) Optimal choice $(\beta^*, \hat{\beta}^*)$ of the control gains as a function of the additional delay $\hat{\sigma}$ (solid curves), and the choice $(\beta_J^*, \hat{\beta}_J^*)$ suggested by the cost function-based design via (21) (dashed curves). (b) Optimal energy consumption per unit mass w^* (solid brown curve) and energy consumption w_J^* of the cost function-based design (dashed brown curve). (c) Optimal cost function J^*.

one at the upper left corner and one in the middle. When $\hat{\sigma} < \hat{\sigma}_{\rm cr}$, see Fig. 4(a,b), the top left local minimum becomes the global optimum; while for $\hat{\sigma} > \hat{\sigma}_{\rm cr}$, see Fig. 4(c,d), the local minimum in the middle becomes the global optimum. Apart from this sudden change, the optimal gains $(\beta^*, \hat{\beta}^*)$ plotted in Fig. 5(a) show robustness, since there are slight variations only when $0 \leq \hat{\sigma} < \hat{\sigma}_{\rm cr}$ or $\hat{\sigma} > \hat{\sigma}_{\rm cr}$.

The corresponding optimal energy consumption w^* is depicted as a function of the additional delay $\hat{\sigma}$ by solid brown curve in Fig. 5(b). Indeed, there is a minimum at a nonzero additional delay value (marked by the black dot). The optimal set of parameters is identified as $(\beta^*, \hat{\beta}^*, \hat{\sigma}^*) = (0.3, 1.1, 3.7)$, while the optimal energy consumption is $w^* = 3.06$ [kJ/kg]. This is 18.0% less than the optimum of ACC and 3.0% less than the optimum of CCC without additional delay.

However, $(\beta^*, \hat{\beta}^*, \hat{\sigma}^*)$ may not be available online in practice, as finding it requires exhaustive brute force numerical simulations over the parameter space $(\beta, \hat{\beta}, \hat{\sigma})$. The cost function J introduced in (21) can avoid the simulation while still perform the parameter search. The dashed curves in Fig. 5(a) show gains $(\beta_J^*, \hat{\beta}_J^*)$ that minimize the cost function J, whose minimal value J^* is plotted in Fig. 5(c). The optimal gains $(\beta_J^*, \hat{\beta}_J^*)$ show robustness against the delay $\hat{\sigma}$ and approximate the results $(\beta^*, \hat{\beta}^*)$ of numerical simulations for $\hat{\sigma} > \hat{\sigma}_{\rm cr}$. The energy consumption w_J^* corresponding to $(\beta_J^*, \hat{\beta}_J^*)$ is close to the actual w^* associated with $(\beta^*, \hat{\beta}^*)$, as shown by the dashed brown curve in Fig. 5(b). The parameters minimizing J are $(\beta_J^*, \hat{\beta}_J^*, \hat{\sigma}_J^*) = (0.3, 0.95, 4.2)$ with energy consumption $w_J^* = 3.09$ [kJ/kg]; see the blue points in Fig. 5(b,c). The optimal parameters and energy consumption of the various control designs are summarized in Table II. These results are practically achievable while being close to the results of numerical simulations.

TABLE II

COMPARISON OF VARIOUS CONTROL DESIGNS.

	$\hat{\sigma}$[s]	β[1/s]	$\hat{\beta}$[1/s]	w[kJ/kg]	Energy Saved
ACC	-	0.65	-	3.73	-
CCC	0	0.05	1.95	3.16	15.4%
	3.7	0.30	1.10	3.06	18.0%
	4.2	0.30	0.95	3.09	17.2%

To understand the reason behind additional energy saving, in Fig. 6 we show the simulation results for (1,6) with the optimal parameters $(\beta^*, \hat{\beta}^*, \hat{\sigma}^*)$ and $(\beta_J^*, \hat{\beta}_J^*, \hat{\sigma}_J^*)$, as the black and blue curves, respectively. We also plot two benchmark scenarios: ACC in pink and CCC with $\hat{\sigma} = 0$ in brown. The proposed control design with the additional delay leads to smoother velocity profile and eliminates abrupt acceleration and deceleration. In addition, the proposed algorithm maintains a smaller average headway compared to the benchmark, i.e., the energy benefits do not compromise the capacity of the traffic flow.

Finally, we investigate the effect of having connectivity with different leading vehicles (i.e., having different L). So far, we have assumed that the CAT responds to leading vehicle 8. In practice, however, the number of vehicles between the CAT and the leading CHV (the value of L) may not be available. Fig. 7 depicts w^* and w_J^* as a function of $\hat{\sigma}$ for leading vehicles ranging from vehicle 2 to vehicle 8, i.e., $L = 2, 3, \ldots, 8$. When the CAT responds to vehicles farther ahead (shown by larger L), the overall energy consumption is lower. This can be explained by the string instability of human drivers as the data of vehicles closer to the CAT have larger speed fluctuations than the vehicles in the distance. On

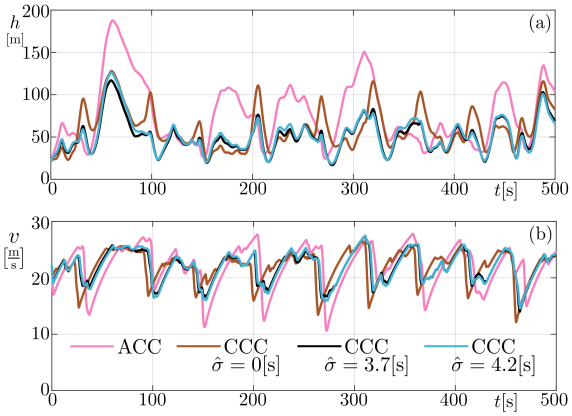

Fig. 6. Simulation results with a heavy-duty truck following preceding vehicle 1 and leading vehicle 8. Pink curve correspond to ACC with optimal parameter $\beta = 0.65\,[1/\text{s}]$, which only involves response to the preceding vehicle. Brown and black curves correspond to CCC with optimal parameters $(\beta^*, \hat{\beta}^*)$ and different additional delays: $\hat{\sigma} = 0$ and $\hat{\sigma} = 3.7\,[\text{s}]$, respectively. Blue curve corresponds to the parameters $(\beta^*_J, \hat{\beta}^*_J, \hat{\sigma}^*_J)$ obtained from optimizing the cost function J. The parameters of the simulation are listed in Tables I and II. (a) Headway profiles. (b) Velocity profiles.

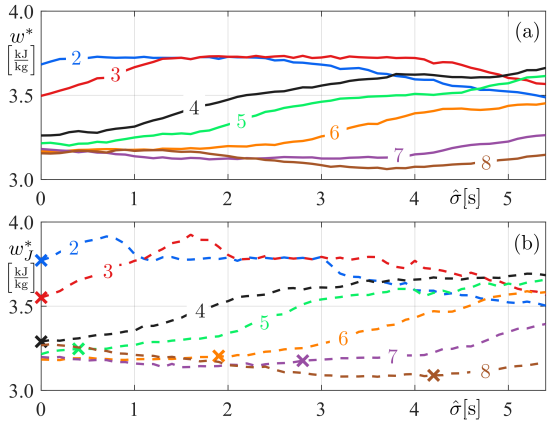

Fig. 7. Energy consumption per unit mass w with leading vehicle ranging from vehicle 2 to vehicle 8. (a) Optimal w^* and (b) suboptimal w^*_J with parameters obtained by optimizing the cost function J. Crosses correspond to delay $\hat{\sigma}^*_J$ that optimize the cost function J.

the other hand, the crosses in Fig. 7(b), which correspond to the delay $\hat{\sigma}^*_J$ minimizing the cost function J, show that the additional delay may be beneficial only if the leading CHV is far enough (i.e., $L \geq 5$ in this example). Finally, responding to vehicles farther ahead (having larger L) is associated with larger optimal additional delay $\hat{\sigma}^*_J$. In summary, the proposed cost function J allows one to estimate the optimal parameters, regardless the value of L.

V. Conclusion

In this paper, we proposed an energy-optimal longitudinal controller for connected automated trucks in mixed traffic with lean penetration of connected vehicles. The controller relies on the position and speed of the vehicle immediately ahead of the truck and the speed of at least one connected vehicle traveling farther ahead, which is obtained by vehicle-to-vehicle communication, and uses delayed information about the motion of the distant vehicle. We used a data-driven approach to optimize controller parameters for energy consumption. The simulation results based on real data showed that even when only one vehicle is connected to the truck a significant improvement in energy efficiency can be achieved. When this connected vehicle is far ahead, using delayed information brings additional energy benefit, while control parameters are robust against the introduction of the additional delay. Investigating the robustness with increasing penetration rates of connected vehicles is left for future research.

References

[1] U.S. Department of Transportation, "2017 commodity flow survey," 2020, data retrieved from US Census Bureau.

[2] A. Hooper and D. Murray, "An analysis of the operational costs of trucking: 2019 update," 2019, American Transportation Research Institute.

[3] United States Environmental Protection Agency, "Fast facts on transportation greenhouse gas emissions," 2018.

[4] A. Sciarretta, G. De Nunzio, and L. L. Ojeda, "Optimal ecodriving control: Energy-efficient driving of road vehicles as an optimal control problem," *IEEE Control Systems Magazine*, vol. 35, no. 5, pp. 71–90, 2015.

[5] C. R. He, H. Maurer, and G. Orosz, "Fuel Consumption Optimization of Heavy-Duty Vehicles With Grade, Wind, and Traffic Information," *Journal of Computational and Nonlinear Dynamics*, vol. 11, no. 6, p. 061011, 2016.

[6] C. R. He, A. Alan, T. G. Molnár, S. S. Avedisov, A. H. Bell, R. Zukouski, M. Hunkler, J. Yan, and G. Orosz, "Improving fuel economy of heavy-duty vehicles in daily driving," in *Proceedings of the American Control Conference*. IEEE, 2020, pp. 2306–2311.

[7] G. Orosz, J. I. Ge, C. R. He, S. S. Avedisov, W. B. Qin, and L. Zhang, "Seeing Beyond the Line of Site – Controlling Connected Automated Vehicles," *Mechanical Engineering*, vol. 139, no. 12, pp. S8–S12, 2017.

[8] T. Ersal, I. Kolmanovsky, N. Masoud, N. Ozay, J. Scruggs, R. Vasudevan, and G. Orosz, "Connected and automated road vehicles: state of the art and future challenges," *Vehicle System Dynamics*, vol. 58, no. 5, pp. 672–704, 2020.

[9] A. Vahidi and A. Sciarretta, "Energy saving potentials of connected and automated vehicles," *Transportation Research Part C*, vol. 95, pp. 822–843, 2018.

[10] C. R. He, J. I. Ge, and G. Orosz, "Fuel efficient connected cruise control for heavy-duty trucks in real traffic," *IEEE Transactions on Control Systems Technology*, pp. 1–8, 2019.

[11] V. Turri, B. Besselink, and K. H. Johansson, "Cooperative look-ahead control for fuel-efficient and safe heavy-duty vehicle platooning," *IEEE Transactions on Control Systems Technology*, vol. 25, no. 1, pp. 12–28, 2017.

[12] X.-Y. Lu and S. Shladover, "Integrated ACC and CACC development for heavy-duty truck partial automation," in *Proceedings of the American Control Conference*. IEEE, 2017, pp. 4938–4945.

[13] J. I. Ge and G. Orosz, "Connected cruise control among human-driven vehicles: Experiment-based parameter estimation and optimal control design," *Transportation Research Part C*, vol. 95, pp. 445–459, 2018.

[14] J. I. Ge, S. S. Avedisov, C. R. He, W. B. Qin, M. Sadeghpour, and G. Orosz, "Experimental validation of connected automated vehicle design among human-driven vehicles," *Transportation Research Part C*, vol. 91, pp. 335–352, 2018.

[15] G. Orosz, B. Krauskopf, and R. Wilson, "Bifurcations and multiple traffic jams in a car-following model with reaction-time delay," *Physica D*, vol. 211, no. 3, pp. 277–293, 2005.

[16] A. Galip Ulsoy, "Time-delayed control of SISO systems for improved stability margins," *Journal of Dynamic Systems, Measurement, and Control*, vol. 137, no. 4, p. 041014, 2015.

[17] L. Zhang and G. Orosz, "Motif-based design for connected vehicle systems in presence of heterogeneous connectivity structures and time delays," *IEEE Transactions on Intelligent Transportation Systems*, vol. 17, no. 6, pp. 1638–1651, 2016.